

Widespread activation of awake mouse cortex by electrical stimulation

Maria C. Dadarlat¹, Yujiao Sun², and Michael P. Stryker³

Abstract—Electrical stimulation is a highly-effective, temporally-precise technique to evoke neural activity in the brain, and thus is critically important for both research and clinical applications. Here, we set out to understand the time-course and spatial spread of neural activation elicited by electrical stimulation. By imaging the cortex of awake, chronically-implanted, transgenic mice during electrical stimulation, we found that a broad range of stimulation parameters led to widespread neural activation. In general, increasing current amplitude and the number of stimulation pulses progressively produced higher maximum activity and activated larger areas of cortex. However, increasing stimulation frequency above 30 Hz primarily shifted the timing, not amplitude, of peak activity. Our results demonstrate that even weak electrical stimulation widely activates neurons within awake mouse cortex.

I. INTRODUCTION

Electrical stimulation allows experimenters and clinicians to manipulate neural activity, causally linking activity in particular brain areas with cognitive and motor function. Electrical stimulation has been used to evoke perceptions as wide-ranging as visual and somatosensory sensations [1], [2], memories and experiences [3], and motor activity [4]. Given its widespread use, it is surprising how little is known about the extent and dynamics of neural activation by electrical stimulation in awake, behaving animals.

Electrophysiological studies, using pairs of electrodes inserted into (anesthetized) cortex to record activity [5], [6], found that neurons activated by intracortical electrical stimulation have a stereotyped response: given sufficient charge input, electrical stimulation evokes a short burst of spiking followed a longer-lasting inhibition [6].

However, accurately estimating the *spread* of neural activation using this technique has proved difficult, largely due to the technical challenges of sampling from a sufficiently large fraction of the neural population, and because electrophysiological recordings tend to be biased towards high-firing cells.

Optical techniques for recording neural activity, such as two-photon microscopy or widefield imaging, overcome these issues by tracking, in a large population of neurons,

the activity of genetically-encoded fluorescent calcium indicators that reflect neural activity [7]. Widefield imaging is particularly well-suited for accurately estimating the spread of neural activation during electrical stimulation because, despite low temporal resolution, it reports weak signals by pooling together responses from many neurons and, furthermore, simultaneously records from a large portion of the cortex.

In this paper, we set out to use widefield imaging to determine the amplitude and spatial spread of neural activation in *awake, chronically-implanted* animals as a function of the number of electrical stimulation pulses, current amplitude (μA), and stimulation frequency (Hz). Although there has been some work in understanding the spread of neural activation after electrical stimulation in rodents [8], [9], [10], these were done under anesthesia using large currents ($> 10 \mu\text{A}$) and high stimulation frequencies ($> 100 \text{ Hz}$). In contrast, we constrained the stimulation amplitudes and frequencies we used by biological considerations, taking into account previous work that found that animals behaviorally report detection of stimulation currents as low as $6 \mu\text{A}$ [11] and mimicking the low frequency at which neurons in mouse cortex fire (typically less than 100 Hz), a range that is thought to play an important role in many cognitive functions [12].

We found that even very low stimulus strengths drive a widespread neural response in the brain of awake mice.

II. METHODS

A. Surgical procedures

All procedures were conducted in accordance with the ethical guidelines of the National Institutes of Health and were approved by the Institutional Animal Care and Use Committee at the University of California, San Francisco. Five inbred CAMKII-TTA G6-TRE mice aged 3–6 months (both male and female) were used in this study. These mice express a slow fluorescent calcium indicator, GCaMP6s [7], in all excitatory neurons in the brain.

Each mouse underwent a total of three separate surgical procedures in order to implant 1) a titanium headplate, 2) a platinum/iridium (Pt/Ir) electrode (0.1 M Ω , Microprobes for Life Sciences) and a glass cranial window, and 3) a two-pin receptacle connector and ground wire. For each procedure, animals were anesthetized to areflexia using a mixture of Ketamine and Xylazine (100 mg/kg and 5mg/kg, IP). The surgery to implant a titanium headplate was previously described in detail [13]. The headplates used here were modified from the original design by removing the rear third, leaving a semicircular portion with lateral flanges.

¹Maria C. Dadarlat is a Postdoctoral Fellow in the Physiology Department at the University of California – San Francisco, 675 Nelson Rising Lane, Room 436 San Francisco, CA 94158 mdadarla@phy.ucsf.edu

²Yujiao Sun is a Postdoctoral Fellow in the Physiology Department at the University of California – San Francisco, 675 Nelson Rising Lane, Room 436 San Francisco, CA 94158 jsun@phy.ucsf.edu

³Michael P. Stryker is Faculty in the Physiology Department at the University of California – San Francisco, 675 Nelson Rising Lane, Room 415B San Francisco, CA 94158 stryker@phy.ucsf.edu

This research was supported by a UCSF Program in Breakthrough Biomedical Research award CA-0086624 (M.C.D), a NEI K99 award 1K99EY029002-01 (Y.S), and a NIH R01EY02874 (M.P.S).

After allowing the animal to recover for several days, we implanted the Pt/Ir electrode and glass cranial window. The latter was previously described in [14]. The Pt/Ir electrode was implanted at a 7° or 11° angle to a depth of $200\ \mu\text{m}$ below the cortical surface using a micromanipulator. The electrode was implanted at this relatively shallow depth to ensure that the tip could be visualized from the surface. Next, a layer of sterile Vaseline was placed along the posterior of the craniotomy behind which a layer of cyanoacrylate mixed with dental acrylic was added to fix the electrode in place. After the electrode was secure and the Vaseline removed, a 3 mm glass window was placed over the craniotomy. The edges of the window were fixed in place using cyanoacrylate, and were further stabilized by the application of a dental acrylic.

After allowing the animal to recover for several days, a two-pin receptacle connector and ground wire were implanted. First, one pin of the connector was electrically connected to the end of implanted electrode using a conductive silver paint. The connection was insulated using cyanoacrylate, and the rest of the connector was firmly attached to the rear of the titanium headplate using more cyanoacrylate. To complete the circuit, a small hole was drilled through the skull over contralateral frontal lobe. The stripped end of the silver wire was inserted and the opening was covered with a biocompatible silicone elastomer. Finally, cyanoacrylate was applied over the silicone elastomer and over any loose portion of the ground wire to provide further stability and electrical insulation.

B. Optical imaging

Six days to 2 weeks after electrode implantation, mice were placed on a styrofoam ball (20 cm diameter) and allowed to rest or run freely. The animal's head was fixed in place above the treadmill by screwing the headplate into a rigid crossbar, and the imaging macroscope was centered above the glass window (Fig. 1A). First, an image of the surface was taken to verify clarity of the imaging window and locate the tip of the stimulating electrode (Fig. 1C). Then, the camera was focused $400\ \mu\text{m}$ below the surface in order to record responses evoked by electrical stimulation. All imaging sessions took place in a dark room.

The custom-built macrocope that was used is based on the tandem lens design used for intrinsic signal imaging [15] and is similar to that described in [16]. Images were taken at 30 Hz. Stimulation and imaging data were synchronized by UDP signals sent from the computer controlling the stimulator.

C. Electrical Stimulation

Electrical stimulation sessions were performed at least three hours apart. Each stimulation session consisted of 5 repetitions of a set of parameters, delivered in pseudo-random order at a frequency of 0.1 Hz. Sessions would vary either current amplitude ([1, 2, 5, 7, 10, 12, 15] μA ; 100 Hz; 10 pulses), stimulation frequency ([20, 30, 40, 50, 60, 70, 100] Hz; 10 μA ; 10 pulses), or the number of stimulation pulses ([1, 2, 3, 4, 5, 6, 7, 8, 9, 10] pulses; 100 Hz; 10

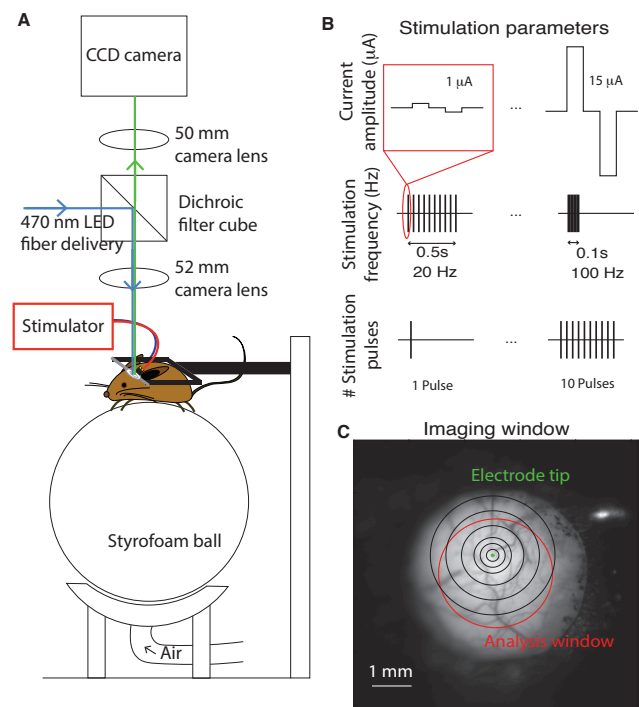


Fig. 1. Imaging and stimulation setup. (A) Physical setup of imaging macrocope and configuration of awake, head-fixed mouse. The mouse is free to run or sit still on a ball floating on a stream of air. The macrocope is centered over the glass imaging window. (B) Schematic depicting the stimulation parameters that were explored: current amplitude (top), stimulation frequency (middle), and the number of stimulation pulses (bottom). (C) The cortical surface imaged through the chronically-implanted glass imaging window. The electrode tip is clearly visible (green dot). Analysis was confined to neural responses within a clear portion of the imaging window, manually selected by the authors for each mouse (red circle). The black concentric circles are centered on the electrode tip and have radii of 0.1, 0.2, 0.3, 0.5, 0.75, and 1 mm.

μA). A single stimulus consisted of a number of biphasic, cathode-first pulses of $200\ \mu\text{s}$ duration (Fig. 1B).

D. Data analysis

Data preprocessing Fluorescent imaging data was analyzed in terms of dF/F , the change in the fluorescent signal from baseline (mean fluorescence in the second preceding stimulation onset from the fluorescent trace), calculated by subtracting the baseline, F_b , and then normalizing the response by that same value: $dF/F(t) = \frac{F(t) - F_b}{F_b}$. Next, to ensure that the analyzed data came from a clear imaging window, the authors used the blood vessel image to choose a crop area (Fig. 1C red circle) and pick the center of the electrode (Fig. 1C green dot).

Evoked responses were analyzed in terms of radial distance from the electrode tip, illustrated in Fig. 1C as a series of black concentric circles at radii of 0.1, 0.2, 0.3, 0.5, 0.75, and 1 mm. The responses within each range were averaged together to form estimates of the relationship between evoked responses and distance from the stimulating electrode. The distances are reported in terms of the radius of the larger circle, e.g. 0.2 refers to the average response in the annulus defined by circles of radius 0.1 and 0.2 mm.

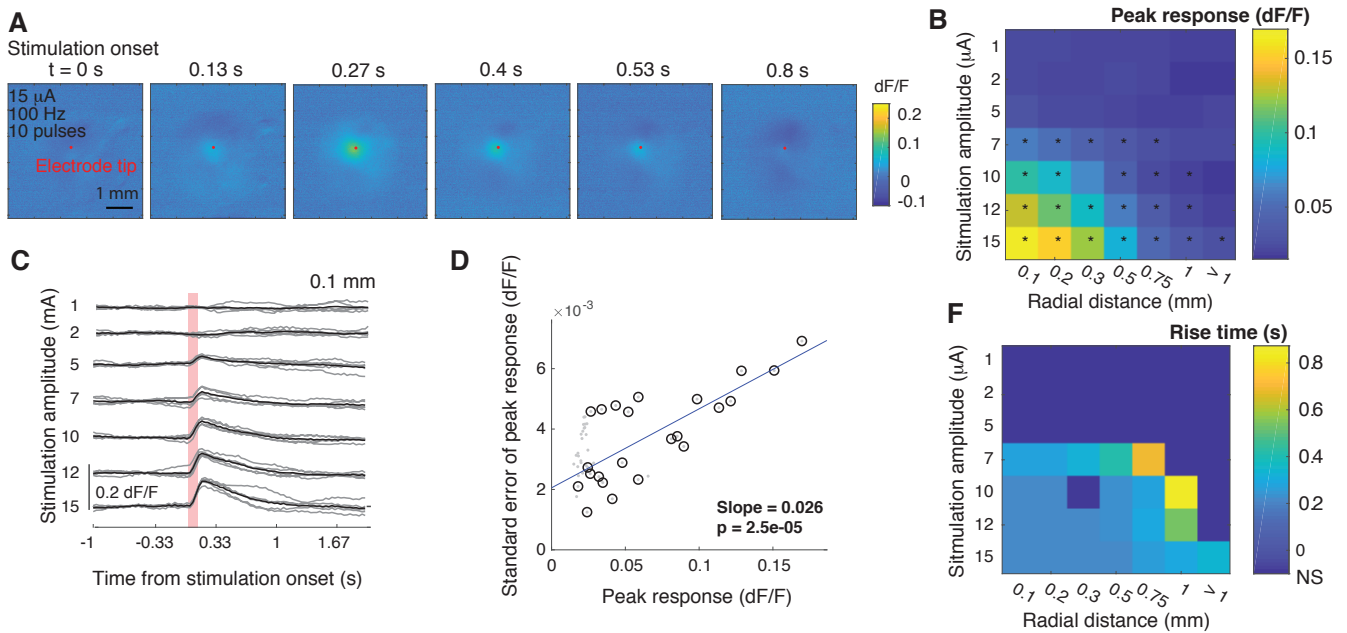


Fig. 2. Current amplitude strongly affects the amplitude and spatial extent of neural activation. (A) Sample images from a single stimulation trial in one mouse depicting evoked neural activity after a stimulus of $15 \mu\text{A}$, 100 Hz , 10 pulses (delivered at $t = 0 \text{ s}$). Color intensity depicted dF/F relative to the one second prior to stimulation onset. The red dot marks the position of the electrode tip. (B) Average peak responses as a function of stimulation current amplitude and distance from stimulating electrode (5 mice). Each distance listed represents the upper limit of a range over which evoked responses were averaged. Stars denote responses that are significantly higher than than spontaneous fluctuations (taken as the responses at $> 1\text{ mm}$ using $1 \mu\text{A}$; $p < 0.001$, Wilcoxon rank-sum test). (C) Single-trial (gray traces) and trial-averaged (black) responses within 0.1 mm from the electrode tip as a function of stimulation current amplitude (sample data from a single mouse). The vertical red bar marks the duration of stimulation (0.1 s , 10 pulses at 100 Hz). (D) Relationship between the amplitude and standard error of peak responses (gray dots). Black circles denote significant evoked responses. Blue line represents the fit of a linear regression between the amplitude and standard error of the significant responses. (E) Average rise-to-peak times as a function of stimulation current amplitude and distance from stimulating electrode (5 mice). Distances represent upper limit of a range. Rise times were calculated only for stimulation amplitudes and distances with significant evoked responses (black stars in (B)).

Peak response and rise time To remove slow fluctuations in fluorescence that were unrelated to stimulation, single-trial response traces were zero-phase digitally filtered (6th-order high pass Butterworth filter with a cutoff frequency of 7 Hz), which distorted the shape but not the time of the peak response. Peak response time was found by taking the time point of the maximum of the filtered response, and the peak response was calculated as the value of the *unfiltered* trace at that time point minus the value of the unfiltered trace at the time of stimulation onset. The rise time was calculated as the difference in between peak response time and stimulation onset.

III. RESULTS

A. Current amplitude

We first measured the spread and amplitude of stimulation-evoked neural activity as a function of stimulating current amplitude in five mice. A train of 10 biphasic pulses at 100 Hz was delivered once every 10 s , with current amplitude taking one of seven possible values: $1, 2, 5, 7, 10, 12, 15 \mu\text{A}$. There were five presentations of each current amplitude, delivered in pseudorandom order.

Electrical stimulation of cortical tissue in awake mice evokes a transient response in the neural population, with a quick rise and a longer decay (Fig. 2A) that likely reflects the slow dynamics of the genetically-encoded fluorescent

calcium indicator, GCaMP6s [7]. To understand how evoked responses vary with stimulation parameters, we analyzed two components of the evoked response: the peak (maximum) of the evoked response and the rise time to peak.

We found that the amplitude of the peak response was highly dependent on stimulation and analysis parameters, growing with current amplitude and falling with radial distance (Fig. 2B, C). Even low-amplitude stimulation significantly activated the population, with a threshold of around $5\text{--}7 \mu\text{A}$ ($p < 0.001$ Wilcoxon rank-sum test, compared to responses at $1 \mu\text{A}$ and 0.1 mm), although this threshold increased with radial distance from the stimulating electrode (Fig. 2B, C). For a given set of parameter values, single-trial evoked-responses were highly reliable, exhibiting low variance in both the amplitude and dynamics of the response (Fig. 2C). In fact, for stimulation parameters that evoked significant responses, response variability was linearly related to the amplitude of the evoked response (linear regression slope of 0.026 , $p = 2e - 5$).

In contrast to response amplitude, we found that rise time was only weakly dependent on stimulation amplitude and distance from the electrode tip, taking a value of 0.23 s for above-threshold values close to the electrode tip. The relative stability of rise times implies that stimulation-evoked neural activity we imaged may result from the *direct* activation of the population of neurons across space. Another possibility is

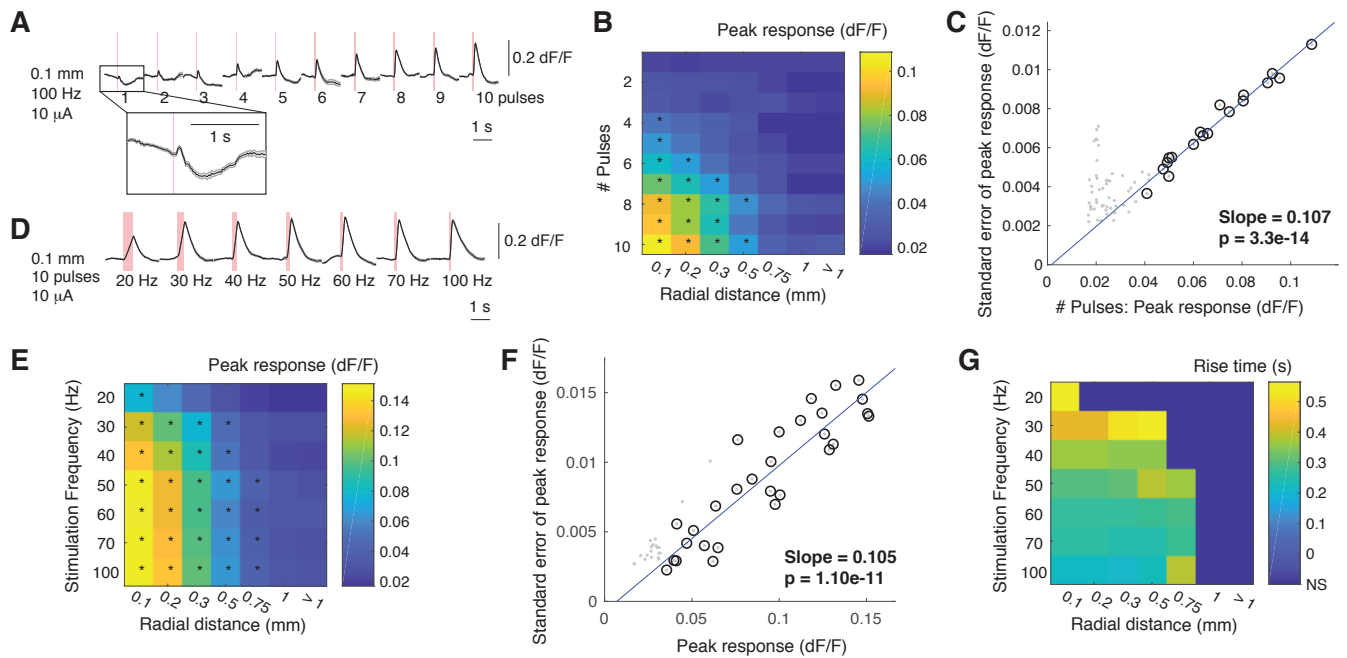


Fig. 3. The number of biphasic stimulation pulses and stimulation frequency both affect the amplitude and spatial extent of neural activation. (A) Average responses from a single mouse at 0.1 mm, plotted as a function of the number of stimulation pulses (10 μ A, 100 Hz). Red bars denote the duration of electrical stimulation. (B) Average peak responses as a function of the number of stimulation pulses and distance from stimulating electrode (5 mice). Each distance listed represents the upper limit of a range over which evoked responses were averaged. Stars denote responses that are significantly higher than than spontaneous fluctuations (taken as the responses at > 1 mm using 1 μ A; $p < 0.001$, Wilcoxon rank-sum test). (C) Relationship between the number of stimulation pulses and standard error of peak responses (gray dots). Black circles denote significant evoked responses. Blue line represents the fit of a linear regression between the amplitude and standard error of the significant responses. (D) Average responses from a single mouse at 0.1 mm, plotted as a function of stimulation frequency (10 μ A, 10 pulses). Red bars denote the duration of electrical stimulation. (E) Average peak responses as a function stimulation frequency and distance from stimulating electrode (5 mice). Each distance listed represents the upper limit of a range over which evoked responses were averaged. Stars denote responses that are significantly higher than than spontaneous fluctuations (taken as the responses at > 1 mm using 1 μ A; $p < 0.001$, Wilcoxon rank-sum test). (F) Relationship between stimulation frequency and standard error of peak responses (gray dots). Black circles denote significant evoked responses. Blue line represents the fit of a linear regression between the amplitude and standard error of the significant responses. (G) Average rise-to-peak times as a function of stimulation frequency and distance from stimulating electrode (5 mice). Distances represent ranges. Rise times were calculated only only for stimulation frequencies and distances with significant evoked responses (black stars in (E)).

that there is a fixed ratio of directly-activated to indirectly-activated neurons (activation by electrical stimulation versus by other, activated neurons) at all distances from the electrode tip. However, the uniformity of rise times may also be an artifact of the combination of a low-resolution measuring system, which is limited to 0.033 s resolution by the 30 Hz sampling rate, and the relatively slow dynamics of the genetically-encoded fluorescent indicator. The slow decay time may also be responsible for masking the post-excitation inhibition that is recorded using electrophysiology [6] but was not observed here.

B. Number of biphasic pulses in the stimulus train

Next, we investigated in three mice how the number of pulses used in the stimulus train shapes the neural activation profile. During the pulse manipulation sessions, current amplitude and stimulation frequency were kept fixed at 10 μ A and 100 Hz respectively. A stimulus of one to 10 pulses at 100 Hz, 10 μ A was delivered once every 10 s. There were five presentations of each pulse number, delivered in pseudorandom order.

In one mouse, a single pulse at 10 μ A was sufficient to evoke a small response (Fig. 3A). In the other two

mice, visible responses emerged with two- and three-pulse stimulation. However, the average evoked responses across all mice were only found to be significant at four pulses (Fig. 3B, $p < 0.001$ Wilcoxon rank-sum test, compared to responses evoked by 1 pulse at 0.1 mm). As was the case for current amplitude, the peak response rose steadily with increasing number of pulses, but fell with distance from the electrode tip. The variability in single-trial peak responses was consistently low and strictly proportional to the amplitude of the peak response for significant responses (Fig. 3C). Finally, rise time was not significantly affected by the number of pulses delivered, although this analysis may suffer from the same issues discussed above.

C. Stimulation frequency

Finally, we examined how stimulation-evoked neural activity depends on stimulation frequency in five mice. A train of 10 biphasic pulses at 10 μ A was delivered once every 10 s, with stimulation frequency taking one of seven possible values: 20, 30, 40, 50, 60, 70, or 100 Hz. There were five presentations of each stimulation frequency, delivered in pseudorandom order.

Electrical stimulation evoked a significant response at all

frequencies (Fig. 3D,E), and the spread of activation grew with increasing stimulation frequency up to 50 Hz (Fig. 3E, $p < 0.001$ Wilcoxon rank-sum test compared to responses evoked by 1 pulse at distances greater than 1 mm). The peak response at 20 Hz was significantly lower than that at higher frequencies, but there was no significant difference in the evoked peak response at higher frequencies ($p < 0.001$, Wilcoxon rank-sum test). The evident jump in activation strength and spread between 20 and 30 Hz stimulation may arise from the important role that gamma rhythms (30 - 90 Hz) play in many cognitive functions [12]. Perhaps this frequency range is particularly effective in driving cortical activity.

The most striking difference from the previous experiments is that stimulation frequency strongly shaped the time-course of neural activation (Fig. 3D). Lower frequencies had a much longer rise time (Fig. 3E), to the point that the activation profile was nearly symmetric at 20 Hz. Clearly, at these lower frequencies, individual pulses must not sum in the way that they do at 100 Hz, and instead each pulse sequentially elicits additional activity. This presents an interesting way to control the time-course of neural activity elicited by electrical stimulation for future research or clinical use.

IV. DISCUSSION

Electrical stimulation of cortical tissue is an effective technique to manipulate neural activity in humans as well as experimental animals, and thus is a useful tool for understanding brain function and providing sensory substitution for neural prostheses. Our main objective here was to determine how electrical stimulation works in alert animals, with a ultimate goal of understanding whether it can be used to create a high-bandwidth communication channel into the brain. In particular, being able to control the amplitude, spatial extent, and timing of evoked neural responses is essential to designing multi-channel patterned stimulation for sensory prostheses.

By performing widefield imaging during electrical stimulation of chronically-implanted, awake mice, we were able to determine how three stimulation parameters (current amplitude, number of stimulation pulses, and stimulation frequency) affected the amplitude, spread, and timing of the evoked neural response. First, we found that the amplitude of the evoked response can be controlled by manipulating two parameters: stimulation amplitude and the number of stimulation pulses – both of which determine the total amount of charge input into the brain. Second, the spatial extent of neural activation can be manipulated by all three stimulation parameters, but getting very local, significant activation was most effectively achieved by limiting the number of stimulation pulses that were delivered. Finally, manipulating stimulation frequency was the most effective way of changing the dynamics of neural activation while maintaining a constant activation strength. Higher frequencies evoked an immediate activation, while lower frequencies resulted in a steady increase in activation strength over the period of stimulation. These results establish important

guidelines for designing patterns of electrical stimulation that could be effective in transmitting information to the brain.

REFERENCES

- [1] A. M. Ni and J. H. R. Maunsell, "Microstimulation Reveals Limits in Detecting Different Signals from a Local Cortical Region," *Current Biology*, vol. 20, no. 9, pp. 824–828, 2010.
- [2] G. A. Tabot, J. F. Dammann, J. A. Berg, F. V. Tenore, J. L. Boback, R. J. Vogelstein, and S. J. Bensmaia, "Restoring the sense of touch with a prosthetic hand through a brain interface," *Proceedings of the National Academy of Sciences*, vol. 110, pp. 18279–18284, Oct. 2013.
- [3] T. W. Berger, R. E. Hampson, D. Song, A. Goonawardena, V. Z. Marmarelis, and S. A. Deadwyler, "A cortical neural prosthesis for restoring and enhancing memory," *Journal of Neural Engineering*, vol. 8, p. 046017, Aug. 2011.
- [4] W. Penfield and E. Boldrey, "Somatic motor and sensory representation in the cerebral cortex of man as studied by electrical stimulation," *Brain*, vol. 60, no. 4, pp. 389–443, 1937.
- [5] S. D. Stoney, W. D. Thompson, and H. Asanuma, "Excitation of pyramidal tract cells by intracortical microstimulation: effective extent of stimulating current," *Journal of neurophysiology*, vol. 31, no. 5, pp. 659–669, 1968.
- [6] S. Butovas and C. Schwarz, "Spatiotemporal effects of microstimulation in rat neocortex: a parametric study using multielectrode recordings," *Journal of neurophysiology*, vol. 90, pp. 3024–39, nov 2003.
- [7] T. W. Chen, T. J. Wardill, Y. Sun, S. R. Pulver, S. L. Renninger, A. Baohan, E. R. Schreiter, R. A. Kerr, M. B. Orger, V. Jayaraman, L. L. Looger, K. Svoboda, and D. S. Kim, "Ultrasensitive fluorescent proteins for imaging neuronal activity," *Nature*, vol. 499, no. 7458, pp. 295–300, 2013.
- [8] T. D. Fehérvári, Y. Okazaki, H. Sawai, and T. Yagi, "In vivo voltage-sensitive dye study of lateral spreading of cortical activity in mouse primary visual cortex induced by a current impulse," *PLoS ONE*, vol. 10, no. 7, 2015.
- [9] D. C. Millard, C. J. Whitmire, C. A. Gollnick, C. J. Rozell, and G. B. Stanley, "Electrical and Optical Activation of Mesoscale Neural Circuits with Implications for Coding," *The Journal of Neuroscience*, vol. 35, no. 47, pp. 15702–15715, 2015.
- [10] S. N. Margalit and H. Slovin, "Spatio-temporal characteristics of population responses evoked by microstimulation in the barrel cortex," *Scientific Reports*, vol. 8, no. 1, pp. 1–14, 2018.
- [11] B. Zaaimi, R. Ruiz-Torres, S. A. Solla, and L. E. Miller, "Multi-electrode stimulation in somatosensory cortex increases probability of detection," *Journal of neural engineering*, vol. 10, p. 056013, oct 2013.
- [12] Buzsáki, György and Wang, Xiao-Jing, "Mechanisms of Gamma Oscillations," *Annu Rev Neurosci*, vol. 35, pp. 203–225, 2012.
- [13] C. M. Niell and M. P. Stryker, "Modulation of Visual Responses by Behavioral State in Mouse Visual Cortex," *Neuron*, vol. 65, no. 4, pp. 472–479, 2010.
- [14] D. A. Dombeck, A. N. Khabbaz, F. Collman, T. L. Adelman, and D. W. Tank, "Imaging Large-Scale Neural Activity with Cellular Resolution in Awake, Mobile Mice," *Neuron*, vol. 56, no. 1, pp. 43–57, 2007.
- [15] V. A. Kalatsky and M. P. Stryker, "New paradigm for optical imaging: Temporally encoded maps of intrinsic signal," *Neuron*, vol. 38, no. 4, pp. 529–545, 2003.
- [16] J. B. Wekselblatt, E. D. Flister, D. M. Piscopo, and C. M. Niell, "Large-scale imaging of cortical dynamics during sensory perception and behavior," *Journal of Neurophysiology*, vol. 115, no. 6, pp. 2852–66, 2016.